Elastin: a representative ideal protein elastomer

D. W. Urry[1,2,3*], T. Hugel[2], M. Seitz[2], H. E. Gaub[2], L. Sheiba[4], J. Dea[4], J. Xu[4] and T. Parker[3]

[1]*University of Minnesota, Twin Cities Campus, BioTechnology Institute, 1479 Gortner Avenue, St Paul, MN 55108-6106, USA*
[2]*Ludwig-Maximilians-Universität, Lehrstuhl für Angewandte Physik, Amalienstraße 54, D-80799 München, Germany*
[3]*Bioelastics Research Limited, 2800 Milan Court, Suite 386, Birmingham, AL 35211-6918, USA*
[4]*Spawar Systems Center, Code D711, San Diego, CA 92152-5001, USA*

During the last half century, identification of an ideal (predominantly entropic) protein elastomer was generally thought to require that the ideal protein elastomer be a random chain network. Here, we report two new sets of data and review previous data. The first set of new data utilizes atomic force microscopy to report single-chain force–extension curves for $(GVGVP)_{251}$ and $(GVGIP)_{260}$, and provides evidence for single-chain ideal elasticity. The second class of new data provides a direct contrast between low-frequency sound absorption (0.1–10 kHz) exhibited by random-chain network elastomers and by elastin protein-based polymers.

Earlier composition, dielectric relaxation (1–1000 MHz), thermoelasticity, molecular mechanics and dynamics calculations and thermodynamic and statistical mechanical analyses are presented, that combine with the new data to contrast with random-chain network rubbers and to detail the presence of regular non-random structural elements of the elastin-based systems that lose entropic elastomeric force upon thermal denaturation.

The data and analyses affirm an earlier contrary argument that components of elastin, the elastic protein of the mammalian elastic fibre, and purified elastin fibre itself contain dynamic, non-random, regularly repeating structures that exhibit dominantly entropic elasticity by means of a damping of internal chain dynamics on extension.

Keywords: atomic force microscopy; acoustic absorption; dielectric relaxation; thermoelasticity; entropic elasticity; β-spiral

1. INTRODUCTION

(a) *Definition of ideal or perfect elasticity*

Ideal elasticity is the property whereby the energy expended in deformation of the elastomer recovers completely on the removal of the deforming force. As the energy expended in deformation is given by the area under the force, f, versus the increase in length, ΔL, curve, a perfectly reversible force–extension curve means complete recovery on relaxation of the energy expended on deformation. Therefore, ideal elastomers exhibit perfectly reversible force–extension curves.

Perhaps our earliest perspective of the mechanism underlying ideal elasticity comes from a fundamental observation concerning rubber elasticity. In the mid-19th century, Joule and Thomson noted a quantitative correlation between the increase in temperature of the elastomer due to stretching and the increase in force due to increasing the temperature (Flory 1968). Thermodynamics provides for the analysis underlying this correlation, and the Boltzmann relationship provides the bridge between experimental thermodynamic quantities and a statistical mechanical description of molecular structures.

Continuing qualitatively with the Joule and Thomson correlation, heat produces motion, and the energy represented by heat distributes into the various available degrees of freedom in the chain molecules comprising the elastomer. Accordingly, the release of heat on stretching correlates with a loss of motion. By means of statistical mechanics, the loss of motion is seen as a decrease in entropy on extension. In addition, should a solvent be essential for elasticity, this requires explicit consideration.

However, there is more to elastomeric force than entropy changes arising from changes in mobility. There is also internal energy, and a proper understanding of elasticity requires the delineation of the internal energy and entropy components of the elastomeric force. As the internal energy component of the elastic force increases, irreversible processes, such as chain breakage, become more probable. Therefore, greater durability results as elastomers become more dominantly entropic and durability becomes a feature of an ideal, or more perfect, elastomer.

(b) *Delineation of internal energy and entropy components of elastomeric force*

The delineation of internal energy and entropy components of elastomeric force can begin with the definition of

the Helmholtz free energy, A, also referred to as the maximal work function,

$$A = E - TS, \tag{1.1}$$

where E is the internal energy, T is the absolute temperature (°K), and S is the entropy for the system. The differential of the maximum work function, dA, can be written to include the work done on an elastomer by application of a force, f, over the change in length, dL, i.e.

$$dA = -PdV - SdT + fdL, \tag{1.2}$$

where P is the pressure, and V is the volume. Writing the partial differential of A in equation (1.2) with respect to length at constant V, T and composition, n, gives

$$(\partial A/\partial L)_{V,T,n} = (\partial E/\partial L)_{V,T,n} - T(\partial S/\partial L)_{V,T,n}, \tag{1.3}$$

but by equation (1.2), $(\partial A/\partial L)_{V,T,n} = f$, such that

$$f = (\partial E/\partial L)_{V,T,n} - T(\partial S/\partial L)_{V,T,n}. \tag{1.4}$$

Accordingly, the force is seen to comprise two components, an internal energy component, f_E, and an entropy component, f_S, i.e.

$$f = f_E + f_S. \tag{1.5}$$

Now it becomes useful to find an expression that will allow experimental estimation of the relative magnitude of the internal energy and entropy components of the force. Following Flory *et al.* (1960), when the functions exist and are continuous, the order of a partial differential does not matter, and it can be shown that $(\partial S/\partial L)_{V,T} = (\partial f/\partial T)_{V,L}$, such that

$$f = (\partial E/\partial L)_{V,T,n} + T(\partial f/\partial T)_{V,L,n}. \tag{1.6}$$

Interestingly, this can be rewritten as

$$f_E/f = -T(\partial \ln[f/T]/\partial T)_{V,L,n}, \tag{1.7}$$

which allows for an experimental estimate of the f_E/f ratio from the slope of a plot of $\ln(f/T)$ versus temperature under conditions of constant V, L and composition, n.

By means of an approximate correction term, the f_E/f ratio is estimated under the more usual experimental conditions of constant P, L and at equilibrium (denoted by subscript eq), e.g. with surrounding solvent, i.e.

$$f_E/f = -T(\partial \ln[f/T]/\partial T)_{P,L,eq} - \beta_{eq}T/[\alpha^3(V_i/V) - 1], \tag{1.8}$$

where $\beta_{eq} = (\partial \ln V/\partial T)_{P,L,eq}$ is the thermal expansion coefficient; α is the fractional increase in length, L/L_i, with the subscript i indicating initial length; and V_i and V are the volumes of the elastomer before and after elongation, respectively (Hoeve & Flory 1962; Dorrington & McCrum 1977). The correction term was derived under the assumption of random-chain networks with a Gaussian distribution of end-to-end chain lengths.

As we will see, a random-chain network comprised of a Gaussian distribution of end-to-end chain lengths between cross-links is neither an accurate structural description of the elastin protein nor of its simpler models. In addition, there are important solvation changes that can occur under experimental conditions. Nonetheless, the insight into the magnitude of the entropic component of the elastomeric force provided by equation (1.8), with experimental estimates of the quantities in the correction

term or when neglecting the correction term altogether, is informative, but only when the temperature range for determination of the slope is chosen carefully.

(c) *Basic statistical mechanical expression for entropy*
(i) *The Boltzmann relationship*

The starting point for the statistical mechanical expressions of entropy is the Boltzmann relationship,

$$S = R\ln W, \tag{1.9}$$

R (1.987 cal deg mole^{-1}) is the gas constant, $R = Nk$, N being Avogadro's number (6.02×10^{23} mole^{-1}) and k the Boltzmann constant (1.38×10^{-16} erg deg K^{-1}), and W is the number of *a priori* equally probable states accessible to the system (Eyring *et al.* 1964). W is the volume in phase space occupied by a particular state of a molecular system. In practice, W becomes the product of partition functions for each of the degrees of freedom of the molecular system. There are $3n - k$ d.f., where n is the number of atoms in the molecule and k is the holonomic constraints on the system. In general, there are three translational and three rotational degrees of freedom, and the remainder are vibrational degrees of freedom. For large-sized molecules, the vibrational degrees of freedom also include motions of rotation (or torsional oscillations) about bonds. Due to the constraints of the elasticity measurement $k = 6$; the ends of the molecules are effectively fixed in space such that there are neither whole molecule translational nor rotational degrees of freedom.

(ii) *Fundamental expression for the change in entropy on extension*

Fortunately, when calculating entropic contributions to the elasticity, interest centres on the change in entropy on extension from a relaxed, S^r, to an extended, S^e, state of the elastomer,

$$\Delta S = (S^e - S^r) = R\ln(W^e/W^r). \tag{1.10}$$

As the change in entropy is a ratio, it becomes relatively straightforward to calculate the contribution to the change in entropy of a particular expression of motion accessible to the representation of the molecular structure under examination in its relaxed and extended states. For our purposes the β-spiral structure of the (Gly–Val–Gly–Val–Pro)$_n$, or poly(GVGVP), model of elastin is used and two different means of representing that structure are considered. The first is the enumeration of states in configuration ($\phi - \psi$ torsion angle) space within a given energy cut-off, or weighted by the Boltzmann distribution, for relaxed and extended states, and the second is to use the molecular dynamics approach to determine the change in root mean square (rms) torsional oscillations that occur on extension by the same amount as used in the enumeration of states approach. The magnitudes of the calculated entropy changes on extension obtained by each approach can then be compared.

(d) *Historical notes of proposed mechanisms for the entropic elasticity of elastin*
(i) *Classical (random chain network) theory of rubber elasticity*

During the last half of the last century, identification of ideal (dominantly entropic) protein elasticity required (by
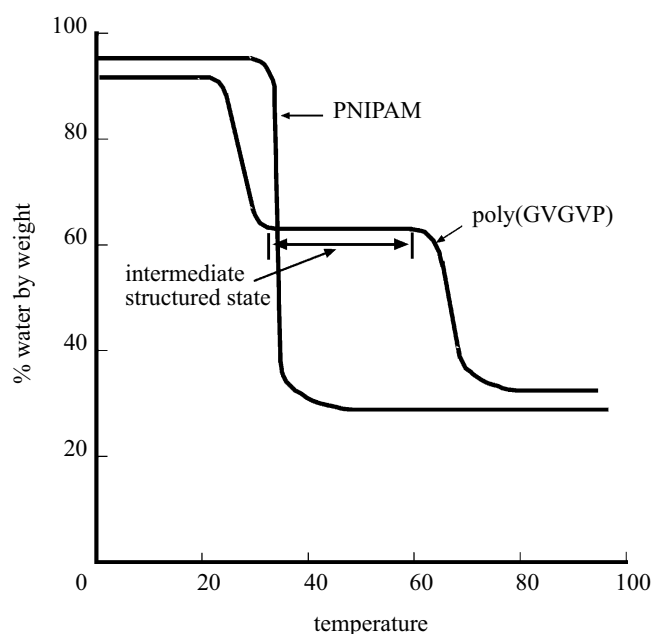
Figure 1. Plot of the percentage water by weight as a function of temperature for poly(GVGVP) showing a stable intermediate structured state of 63% water by weight between 30 °C and 60 °C, a state that slowly denatures above 60 °C to form a state containing 32% water by weight. Graph plotted from the data of Urry *et al.* (1985*b*). Amphiphilic LCST polymers such as PNIPAM, exhibit only a single, sharper transition, to what is generally considered a disordered state, with *ca.* 30% water by weight. Curve plotted from the data of Grinberg *et al.* (1999).

the recognized authorities of the period) the conclusion that the ideal elastomer comprised of random chain networks with a Gaussian distribution of end-to-end chain lengths between cross-links. For elastin, the protein of interest here, this point of view began with a paper by Hoeve & Flory (1958). This perspective became entrenched in the minds of the interested scientific community by the award, in the autumn of 1974, of the Nobel Prize to Paul Flory following reaffirmation of the random-chain network conclusion (Hoeve & Flory 1974). The message of the paper is unmistakable. In the synopsis (p. 677) it is stated, 'A network of random chains within the elastic fibres, like that in a typical rubber, is clearly indicated.' Furthermore, in fig. 1 on p. 678 of their paper there is a structural representation of the chains between cross-links with a statement in the figure legend that, 'Configurations of chains between cross-linkages are much more tortuous and irregular than shown.'

(ii) *Decrease in solvent entropy (due to hydrophobic hydration) on extension*

The purpose of the Hoeve & Flory (1974) paper, which presented no additional data, was to refute an earlier publication by Weis-Fogh & Andersen (1970), which had suggested an alternative mechanism for the elasticity of elastin. The alternative mechanism proposed that hydration of hydrophobic side chains of the protein, which become exposed to solvent on extension, would be responsible for the stretch-induced decrease in entropy,

i.e. by this proposal changes in solvent entropy became the source of the entropic component of the elastomeric force.

(iii) *Damping of internal chain dynamics on extension*

Just over a decade later yet another perspective was put forward. Considering structural studies and molecular mechanics calculations of the most prominent repeating sequence of bovine elastin, $(Gly–Val–Gly–Val–Pro)_{11}$, entropic elasticity was described as arising from a decrease in available configuration space on extension (Urry *et al.* 1982). Equivalently, treating the experimentally and computationally derived regularly repeating structure from the perspective of molecular dynamics, the damping of internal chain dynamics on extension described the same decrease in entropy for the same degree of extension (Chang & Urry 1989).

In § 4, these three mechanisms are considered in more detail, following consideration of new experimental data on models of elastin together with previously published relevant data.

(e) *Inverse temperature transition behaviour of elastin and its models*

(i) *Increase in order with increase in temperature*

Filament formation on raising the temperature

When the temperature of an aqueous solution of the precursor protein, tropoelastin, is increased, the protein aggregates to form a denser viscoelastic phase, called a coacervate. When a droplet of the aqueous suspension of incipient aggregates is placed on a carbon-coated grid, negatively stained with uranyl acetate and oxalic acid at the appropriate pH, and examined under TEM, fibrils comprised of parallel-aligned filaments are observed with a 5 nm periodicity (Cox *et al.* 1974). Similar results are obtained for α-elastin, a 70 000 Da fragment of the elastic fibre (Cox *et al.* 1973), for high polymers, poly(GVGVP) and poly(GVGVAP) of repeating sequences of elastin (Volpin *et al.* 1976). Fibrils of similar dimensions have been reported for fibrous elastin itself using similar techniques (Gotte *et al.* 1974).

Crystallization of cyclic analogues on raising the temperature

Most strikingly, cyclic analogues of repeating sequences of elastin crystallize on raising the temperature (Urry *et al.* 1978; Cook *et al.* 1980) and redissolve on lowering the temperature. Without ambiguity, these polymers increase order with increase in temperature through a transition temperature range.

We refer to this phase transition as an *inverse temperature transition*. While the peptide component of this water–peptide system increases in order on increasing the temperature, ordered water molecules surrounding hydrophobic residues become less-ordered bulk water as hydrophobic groups separate from solution. Accordingly, the overall change effected by the phase transition is towards less order, in keeping with the second law of thermodynamics.

Indeed, the phase diagram for HMW polymers of repeating sequences of elastin is inverted with the soluble phase below, at lower temperature, and the insoluble phase above the binodal or coexistence line and with an inverted coexistence line, i.e. with the curvature of the coexistence line convex to the volume fraction axis

(Sciortino *et al.* 1993; Manno *et al.* 2001). Conversely, the usual circumstance for polymers is for the coexistence line to be concave to the volume fraction axis and for the polymer to be insoluble below and soluble above the coexistence line (Flory 1953).

(f) *Composition of poly(GVGVP) in water as a function of temperature*

The temperature dependence of composition of the poly(GVGVP)–water system provides a clear visualization of a water-containing, structured state at intermediate temperatures (Urry *et al.* 1985*b*). Figure 1 schematically illustrates the plot of percentage water by weight as a function of temperature. As the polymer is miscible with water in all proportions below 20 °C, the plot arbitrarily starts at *ca*. 90% water by weight near 0 °C. A rise in temperature from 20 to 30 °C causes a reversible phase separation to form a state that is 63% water by weight. The percentage water by weight of this intermediate water-retaining state remains essentially unchanged until the temperature rises above 60 °C. Then a very slow irreversible transition occurs on raising the temperature from 60 to 80 °C to form a state that is 32% water by weight. Dialysis of the polymer against 100 000 molecular weight cut-off membranes, after prolonged heating at 80 °C, resulted in a less than 1% loss of polymer. Prolonged heating did not result in chain breakage, and therefore, the slow irreversible transition was not due to chain breakage.

In figure 1, the results on poly(GVGVP) are compared to those of Grinberg *et al.* (1999) on the petroleum-based polymer, PNIPAM. This polymer shows an inverted phase diagram like that of the elastin-based polymers. Though with a composition more hydrophobic than that of poly(GVGVP), the transition for this LCST polymer occurs at a higher temperature (34 °C), is much sharper, and results directly in the formation of the state with *ca*. 30% water by weight. A reasonable description of this PNIPAM state of 30% water by weight is as a random-chain network. It is clear that poly(GVGVP) forms an intermediate, water-containing state that holds a fixed amount of water until irreversible denaturation occurs at high temperature. This state of 63% water by weight is an elementary property that simply is not consistent with the recently computed 'compact amorphous globule' for (GVGVP)$_{18}$ attributed to Li *et al.* (2000).

(i) *A structured state at intermediate temperatures for elastin-based systems*

Both the elastin fibre and α-elastin at intermediate temperatures form similar water-containing states of *ca*. 50% water by weight (Partridge *et al.* 1955; Partridge & Davis 1955; Partridge 1966, 1967). It will also be demonstrated below (see figure 8) that both cross-linked poly(GVGVP) and fibrous elastin exhibit a slow, irreversible, loss of elastic force due to prolonged exposure to temperatures above 60 °C when at fixed extension. These are further demonstrations of the slow irreversible denaturation observed in figure 1, that occurs above 60 °C, for poly(GVGVP). Furthermore, detailed dielectric relaxation studies on the elastin-based systems—fibrous elastin, α-elastin, and poly(GVGVP)—demonstrate molecular motions, relaxations, limited to localized frequency ranges (see figures 6 and 7), and these could only be the result of non-random,
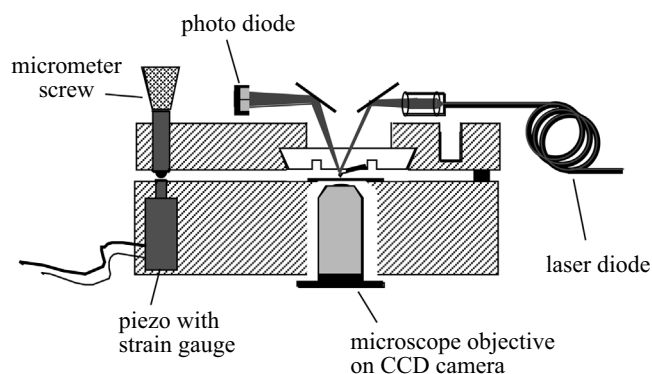

Figure 2. Schematic diagram of an AFM apparatus adapted for varying the *z*-direction to obtain force–extension curves for single chains.

regularly structured, albeit dynamic, conformational states. These experimental results are not consistent with random-chain networks nor are they consistent with compact amorphous globules.

2. MATERIAL AND METHODS

(a) *Preparation of elastin models*

In the native state of elastin, the precursor, tropoelastin, a protein of about 70 000 Da, occurs as the overwhelmingly dominant component (90+% by weight) of the mammalian elastic fibre. In the vascular wall, for example, the elastic fibre resides within the extracellular matrix as a structure several microns in diameter. No functional role is given to non-elastin components within the elastic fibre. During cross-linking by the enzyme, lysyl oxidase, it can be trapped within the fibre, and a fine coating of microfibres, some hundreds of nanometers in thickness, can surround the fibre. Due to the cross-linking, elastin is an insoluble material of the extracellular matrix. Efforts to isolate it, in order to define its properties, require Draconian methods. For example, refluxing in sodium hydroxide, denaturants and proteolytic enzymes are used to remove all of the surrounding matrix components. This insoluble product is called purified fibrous elastin.

Alternatively, for the study of elastin, model approaches have been used such as isolating and characterizing (i) the precursor protein, tropoelastin, which may be obtained in ill-defined intermediate states of cross-linking, (ii) the pure precursor protein prepared by microbial biosynthesis, (iii) chemical degradation products of purified fibrous elastin which have been prepared, and (iv) chemically and microbially synthesized repeating sequences found within the protein sequence as well as interesting analogues which have been prepared.

(i) *Synthesis of model systems*
Chemical synthesis

Initially, several thousand protein-based polymers were synthesized in order to determine the conformation and function of these model proteins. This involved the synthesis of oligomers and high polymers of repeating tetra-, penta-, hexa-, nona- and even decapeptides reported in the sequence of elastin. By means of chemical synthesis, many compositions could be prepared and characterized, and axioms were developed for the function of these elastic model proteins in energy conversion and for their use as biomaterials for medical and non-medical applications.
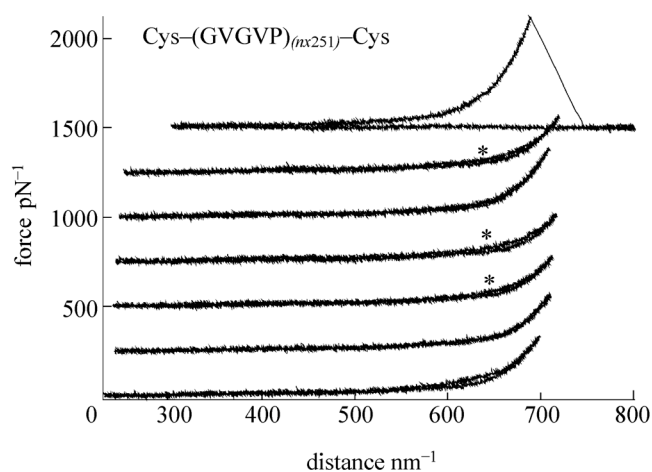
Figure 3. Single-chain force–extension curves for Cys–(GVGVP)$_{nx251}$–Cys at a temperature below the onset temperature for hydrophobic folding and assembly for this composition. The initial trace appears at the lowest position on the graph and subsequent traces of the same chain, without intervening detachment, are displaced 250 pN vertically. The second and fifth curves exhibit perfect reversibility. The curves marked by an asterisk, and the initial curve, were the result of a period of at least 30 s in the relaxed state, where one possibility is that some hydrophobic back folding occurs.

Microbial biosynthesis

Once a specific composition was identified as being of sufficient interest, it was prepared by means of recombinant DNA technology. With this approach, hundreds of grams could be prepared in a single fermentation. On the other hand, chemical synthesis at the laboratory bench would require much of a year to prepare such a quantity.

(ii) *Preparation of natural materials*
Isolation of the precursor protein, tropoelastin

Initially, the precursor protein was prepared from animals rendered copper deficient and treated with inhibitors of enzymatic cross-linking. The product was meagre in amount and a mixture of partially cross-linked and oxidized lysyl side chains. It was nonetheless helpful in determining many of the fundamental physical properties relating to structure and elastogenesis.

Preparation of tropoelastin by microbial biosynthesis

In an important development, Weiss and co-workers utilized recombinant DNA technology to prepare the precursor protein, tropoelastin, in *Escherischia coli*, which enabled the preparation of pure protein in large quantities (Vrhovski *et al.* 1997; Wu *et al.* 1999). Important aspects deduced by the model systems and by preparations of model structures derived from the elastin and from sequence knowledge have been confirmed and extended by recombinantly prepared tropoelastin.

Preparation of α-elastin

A model system useful in stepping systematically from polymers of model-repeating sequences to the natural fibrous elastin has been a chemical fragmentation product from fibrous elastin called α-elastin, prepared and chemically characterized by Partridge and co-workers (Partridge *et al.* 1955; Partridge & Davis 1955; Partridge 1966, 1967). It is a multiply cross-linked, 70 000 molecular weight fragment comprising 16 chains.

(iii) *Purification using phase transitional behaviour*

In all cases these protein-based polymers are soluble in water at a lower temperature and phase separate on raising the temperature above that for the onset of a hydrophobic folding and assembly transition. This phase separation process has been termed coacervation. It is a fundamental property of these polymers having, as they do, the proper balance of apolar (hydrophobic) and more polar residues.

(b) *Cross-linking of elastin models*
(i) *General cross-linking procedure*

Cobalt 60 γ-irradiation was used to cross-link the phase-separated, coacervate state with its interpenetrating polymer chains.

(ii) *Efforts to cross-link α-elastin*

Even though α-elastin undergoes phase separation, it does not form an elastic matrix on γ-irradiation. As a cluster of some 16 cross-linked chains, with a total molecular weight of 70 kDa, α-elastin does not cross-link by γ-irradiation because the cluster of chains of one α-elastin molecule does not interpenetrate sufficiently with surrounding molecules. This is in contrast with similar molecular weights of poly(GVGVP) which readily cross-link by γ-irradiation when in the intermediate structured state between 30 and 60 °C.

(iii) *Efforts to cross-link heat denatured poly(GVGVP)*

While the phase-separated state of poly(GVGVP) with 63% water by weight (figure 1) cross-links very effectively, the heat-denatured state obtained on prolonged heating above 60 °C does not. Even though the density of chains is twice as great for the denatured state formed above 60 °C (a state of 32% water by weight as seen in figure 1), the chains no longer interpenetrate and associate sufficiently to result in an elastic matrix on γ-irradiation. This is simply another demonstration that the intermediate state, between 30 and 60 °C, is a structured state of interpenetrating filaments rather than being globular structures with limited contact between units, as occurs with α-elastin or as would be the case for amorphous compact globules.

3. SPECIALIZED METHODOLOGIES AND ANALYSIS OF RESULTS

(a) *Single molecule force-extension curves by AFM*
(i) *Preparation of the sample for AFM*

Cleaned glass microscope slides were coated with *ca.* 30 nm of gold in a home-built evaporation chamber. Si_3N_4 AFM tips were used (Microlevers, Park Scientific Instruments, Sunnyvale, CA), also coated with gold. For the preparation of mixed self-assembled monolayers, quantities of 1 mg of the polypentapeptides and 0.5 mg of methoxy-PEG-thiol (M_W 5000) were dissolved in 1 ml Milli-Q water unless otherwise noted. A 20 μl portion of this solution was incubated on the gold-coated slide for about 30 min at 3 °C and then rinsed with Milli-Q water.

(ii) *The AFM instrument*

A detailed description of the AFM force spectroscopic technique and details of the instrumental set-up have been supplied elsewhere (Oesterhelt *et al.* 1999; Clausen-Schaumann *et al.* 2000). Briefly, the tip of a cantilever is brought into contact with molecules on the surface and then retracted, its deflection, and therefore the force, are

detected with a laser by optical lever detection (Cleveland *et al.* 1993), while the *z*-distance is controlled by a strain gauge (figure 2). The nominal spring constants of cantilevers used in the experiments were 10 mN m^{-1}. Before the first approach of the AFM tip to the surface, the spring constants of each lever were individually calibrated by measuring the amplitude of their thermal oscillations (Butt & Jaschke 1995). The sensitivity of the optical lever detection was measured by indenting the AFM tip into a hard surface. All experiments were conducted in Milli-Q water at room temperature (21 °C), unless otherwise specified.

(iii) *Obtaining the single-chain force–extension curve*

For the characterization of elastic properties, the gold-coated AFM tip was brought into contact with the polypentapeptides on the microscope slide by manual control. The AFM tip and the polymer layer were kept in contact under a contact force of several nanoNewtons for *ca.* 30 s to allow for an attachment of polypeptide chains to the tip. Usually, one or several chains adsorbed non-covalently at some position on the tip, possibly a chemical reaction between the gold-coated cantilever and the cysteine on the end of a polypentapeptide sometimes allowed for very high rupture forces. Upon retraction of the cantilever, individual polypentapeptides were stretched between the surface and the AFM tip.

Note that the first force–distance profile recorded after tip–substrate contact can be rather complex, consisting of contributions from stretching several polypentapeptides, desorption from the substrate and/or cantilever, bond rupture of short strands, as well as interchain aggregation and entanglements. Therefore, in each measurement the cantilever was first retracted from the substrate to a distance at which unspecific adhesion was no longer observed. Then, in successive retraction-approaching cycles the distance range was increased while trying to avoid contact between the tip and additional polypentapeptide strands at the substrate surface, until only one polymer strand remained between the tip and the substrate. The force–distance profile of this strand was then measured repeatedly until rupture.

(iv) *Analysis of the results*

The experimental traces were fitted by an extended WLC model (Bustamante *et al.* 1994; Odijk 1995) including linear elastic contributions arising from the stretching of bond angles and covalent bonds:

$$F \times \frac{L_P}{k_B T} = \frac{R_z}{L} - \frac{F}{K_0} + \frac{1}{4(1 - R_z/L + F/K_0)^2} - \frac{1}{4}. \quad (2.1)$$

In this expression, R_z is the measured end-to-end-distance at any given force, F, and L is the contour length of the stretched chain (polypentapeptide) under zero force ($F = 0$). It should be appreciated that the WLC model entirely neglects any discrete molecular structure along the chain, and describes the polymer as a continuous rod of constant bending module. The characteristic length scale expressing the polypeptide's bending rigidity is the persistence length, L_P, which is defined as the decay length of the directional correlation along the polymer chain. Finally, the chain's extensibility upon stretching is described by the segment elasticity, K_0, which is intro-

duced into equation (2.1) as a linear term. Hereby, K_0 can be understood as the inverse of the normalized compliance of a Hookean spring; the spring constant of the polymer chain is given by K_0/L.

This resulted in values for the persistence length L_P of $(GVGVP)_{nx251}$: $L_P = 0.4$ nm in the low force regime and $L_P = 0.6$ nm when fitted to higher forces, which are comparable to values measured previously for other polypeptide backbones, e.g. of proteins (Rief *et al.* 1997). The reversible traces provide evidence for single-chain ideal elasticity, i.e. any molecular processes related to the elongation and relaxation of the polypeptide chains must be fast on the time-scale of the AFM experiment. Apart from the entropic contributions at low forces below *ca.* 20 pN, which are related to the unfolding of the polymer coil ('classical conformational entropy'), it has been previously shown that ideal elastic behaviour in the high force regime may also result from enthalpic bond-angle deformations and configurational changes along the polymer backbone (Rief *et al.* 1997). As will be shown below, additional entropic, and therefore reversible elasticity, in the high forces regime can also arise from backbone torsional movements (rocking), wherein the contribution to the entropic component of the force increases with a decrease in the frequency of the oscillator. Temperature-dependent AFM measurements should allow for a proof of this finding at the single molecule level.

The small deviations from perfect reversibility in traces 3, 4 and 6 of figure 3 (marked by the asterisk) occurred when the chain was held for at least 30 s in the relaxed state. These deviations could have several origins. There could be a configurational transition, e.g. an opening of β-turns and/or hydrophobic interaction, a back folding, between different parts of the chain. The latter is favoured by the observed rate dependence of this non-equilibrium contribution.

The persistence length L_P of $(GVGIP)_{nx260}$ is difficult to determine, when intra- and/or interchain aggregation gives rise to a strong hysteresis even when located far away from the surface within two successive cycles (figure 4). It is determined to exhibit an $L_P = 0.7$ nm, which might be slightly higher than with $(GVGVP)_{nx251}$, but this value lies well within the error range of *ca.* 20%. This strong aggregation of $(GVGIP)_{nx260}$ occurs at the same concentration, at which the aggregation for $(GVGVP)_{nx251}$ is much smaller. This reflects the increase in hydrophobicity due to an additional CH_2 group in GVGIP, which is the only difference with GVGVP. Unfortunately, it is not yet clear whether the aggregation is mainly due to back folding within a single chain or due to association between different chains. This is under investigation.

(v) *Comparison of AFM single-chain and macroscopic elastic moduli*

For the characterization of elastomers at the macroscopic scale, force versus elongation is plotted, but instead of being represented as an actual increase in length, as in figures 3 and 4, elongation is stated in terms of the ratio of the initial length to the extended length. Furthermore, the deformation is generally uniform so that the initial cross-sectional area, A, is used. Therefore, the Young's elastic modulus, Y, is the force, f, times the initial length, L_i, divided by the elongation, L, and the cross-section of the elastomer, that

is, $Y = fL_i/AL$. The units are N m^{-2} or dynes cm^{-2} where N m^{-2} = 10 dynes cm^{-2} and N stands for Newtons. The elastic modulus of 20 Mrad γ-irradiation cross-linked (GVGVP)$_{251}$, i.e. X^{20} (GVGVP)$_{251}$, is 1.6×10^5 N m^{-2}.

In order to utilize the data in figure 3 to obtain an estimate of the single-chain elastic modulus, estimates of the L_i/L ratio and of A are required. Initially, the total number of repeats that are being extended must be deduced. In figure 3, the WLC fit of the force–distance trace shown gives an end-to-end-distance of $L = 733$ nm, which we assume is the fully extended chain. This is too long for a chain of 251 pentamers, but appears to be too short for a chain of 753 pentamers. By elimination of chain lengths with 251 and 753 pentamers, this indicates that the structure would be (GVGVP)$_{2 \times 251}$ giving 502 pentamers, i.e. 2510 residues with a value of 0.29 nm per residue. This is shorter than the usual value of 0.35 nm per residue, which could be due to the presence of a proline residue in every pentamer. This results from the *cis* Val–Pro peptide bond, which introduces a kink in the extended backbone for every pentamer. It should be noted, however, that if all of the β-turns were retained at rupture, the 3×251 chain length could apply with *ca.* 1 nm per pentamer, or just greater than 700 nm. This scenario was not considered because the forces for detachment can be greater than 500 pN, and retention of the β-turn was considered less likely at such forces.

It should also be noted that, in general, one cannot exclude *a priori* the possibility of polypeptides being picked up at any position along the chain due to strong unspecific adsorption. In the case of (GVGVP)$_{nx251}$, however, the simplicity and uniformity of the repeating sequence without the presence of functional groups except, at the very ends of the chain, are expected to limit *strong* unspecific adsorption. Because the polymer length estimated from the WLC fit is sufficiently close to what would be expected for 2×251 proline-containing pentamers it warrants, in our view, proceeding with this assumption.

Perhaps the most significant factor in obtaining a relevant value for the single-chain elastic modulus for comparison to the macroscopic case is the choice of the structure before elongation in order to provide an estimate of an initial length and cross-sectional area. In this regard two quite different initial lengths may be considered, one for the random coil state below the hydrophobic folding transition and another for the β-spiral structure that could only occur above the onset temperature for the hydrophobic folding transition.

Calculation of elastic modulus from AFM data assuming a random coil state for (GVGVP)$_{nx251}$

At temperatures lower than the onset temperature for the hydrophobic folding and assembly transition, the more correct representation of the unstretched single chain would be the random coil state. Based on photon correlation spectroscopic studies, the hydrodynamic diameters of disordered polymeric coils resulting from 502 pentamers (some 200 000 Da molecular weight) below the transition would be *ca.* 18 nm (San Biagio *et al.* 1988). By way of example, at a distance of 378 nm in figure 3, the L_i/L ratio would be 1:20. In this distance range (i.e. between 300 and 500 nm), the slope of the force curve is evaluated as 0.08 ±0.03 pNnm^{-1}. With a slope of 0.08 ±
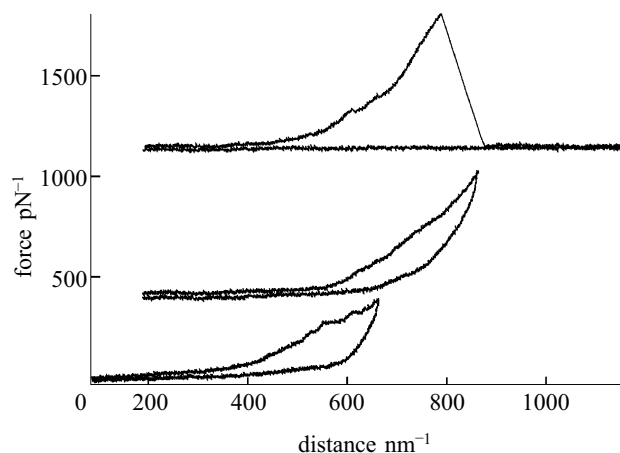

Figure 4. Single-chain force–extension curves for Cys–(GVGIP)$_{nx260}$–Cys at a temperature above the onset temperature for hydrophobic folding and assembly for this composition. In each case the energy expended in deformation is greater than that recovered on relaxation. In addition, there appears to be a complex relaxation curve.

0.03 pN nm^{-1} from figure 3, at a distance of 378 nm from the substrate, the increase in force would be 28.8 ± 10.8 pN; i.e. upon elongation from 18 to 378 nm, the relative increase in length, $\Delta L/L_i$, would be a factor of 20, so that a force of 1.44 ± 0.54 pN is estimated for a 100% extension of the 18 nm diameter polymeric coil.

Next, this quantity should be divided by an appropriate cross-sectional area, that is, π multiplied by the hydrodynamic radius, squared, of the random coil prior to extension of the single chain, i.e. $\pi r^2 = \pi(9 \text{ nm})^2 = 254$ nm^2. Given the foregoing assumptions, the calculated single-chain elastic modulus would be $5.7(\pm 2.1) \times 10^3$ N m^{-2}. As might have been expected, without taking polymer density and cross-link density into consideration (Urry *et al.* 1984), this value is a factor of 30 from the experimental value at 37 °C for X^{20}-(GVGVP)$_{251}$ of 1.6×10^5 N m^{-2}, but more closely approximates what is expected below the transition temperature or when X^{20}-(GVGVP)$_{251}$ has been thermally denatured, as seen in figure 8*b*. Concerning polymer density, it may be noted that the density of the low-temperature random-coil state is about one-quarter that of the phase-separated state.

Calculation of elastic modulus from AFM data assuming the β-spiral structure for (GVGVP)$_{nx251}$

For comparison, it is useful to consider the structure representative of the state above the temperature of the inverse temperature for hydrophobic folding and assembly. This addresses the importance of choosing structure when converting the force–extension curve into a macroscopic elastic modulus. If the single β-spiral structure were assumed before extension with three pentamers per turn and a translation along the axis of 1 nm per turn, the length of a 502 pentamer would be *ca.* 170 nm. This means that an elongation of 100% would occur at 340 nm, and the change in force for extension of the β-spiral from 170 to 340 nm would be 170 nm × 0.08 ± 0.03 pN nm^{-1} = 13.6 ± 5.1 pN per β-spiral.

The next issue is an estimate of the number of β-spirals per m^2 for comparison with the cross-linked matrix from
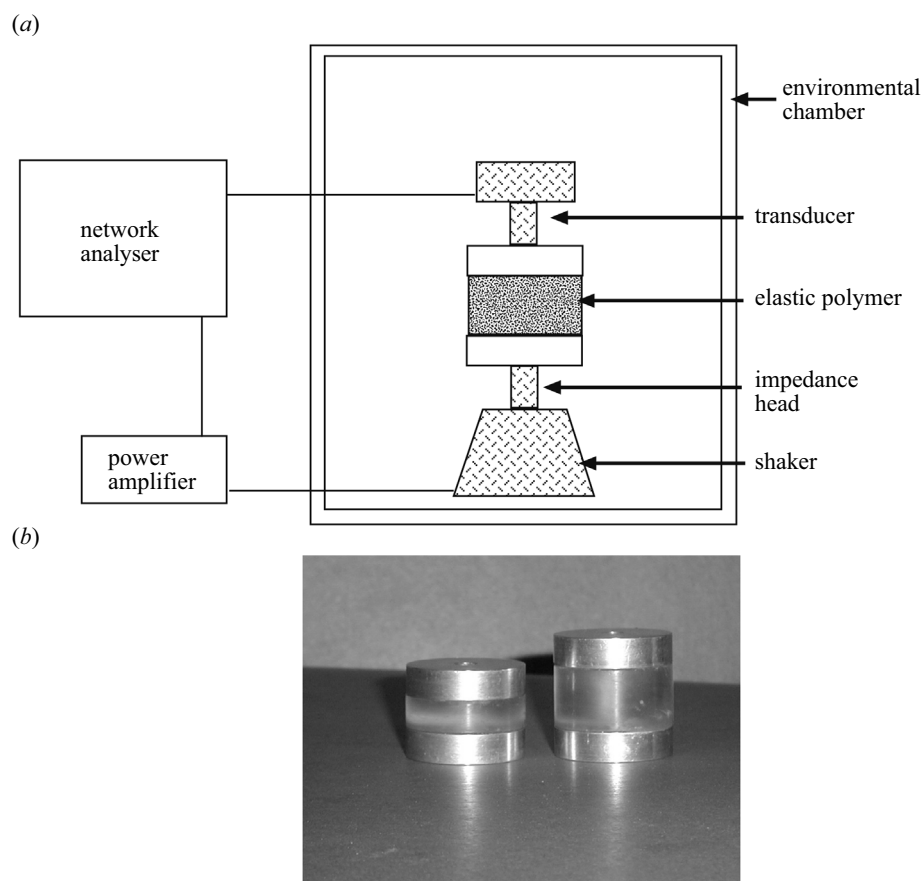
(a)

(b)

Figure 5. (a) Block diagram of the instrumentation used to determine the absorption per unit volume of elastic samples in the acoustic range. (b) Example of the use of two samples that differ in length by a factor of 2 as required to permit the analysis of Sheiba (1996) to be utilized.

which the experimental macroscopic value of $1.6 \times 10^5 \, \mathrm{N \, m^{-2}}$ is obtained. For a macroscopic state of 37% water by weight (see figure 1), an assumed density of $1.33 \, \mathrm{g \, cm^{-2}}$ for the polymer, and a cross-sectional area for the β-spiral of $3.2 \, \mathrm{nm^2}$, the number would be *ca.* 8.7×10^{16} β-spirals $\mathrm{m^{-2}}$. The single-chain elastic modulus, calculated on the basis of the β-spiral structure, would be $(13.6 \pm 5.1 \times 10^{-12} \, \mathrm{N}$ per β-spiral$) \times (-8.7 \times 10^{16}$ β-spirals $\mathrm{m^{-2}}) = 1.2 \times 10^6 \, \mathrm{N \, m^{-2}}$.

Thus, by assuming a different structure, instead of being low by a factor of 30 as was the case above for a random-coil structure, which occurs below the transition temperature, the assumption of the β-spiral structure resulted in a value for the single-chain elastic modulus that is seven and a half times larger than the macroscopic value. We note that the orientation of a random coil is not relevant in the argument relating single-chain data to macroscopic data. For the γ-irradiation cross-linked macroscopic matrix, however, the β-spirals would be randomly orientated with respect to the direction of extension. This would decrease the contribution of each β-spiral not aligned in the direction of extension. It will now be particularly interesting to obtain the elastic modulus for the twisted filament structure depicted in figure 9f. Work is in progress for the preparation of multistranded twisted filaments.

(b) *The acoustic absorption experiment*

(i) *Sample preparation and experimental set-up*

The polymer is prepared in the phase-separated state, i.e. the intermediate structured state with the interpenetrating chains depicted in figure 1, and 20 Mrad γ-irradiation cross-linked in the form of the desired cylindrical shape and with path lengths that differ by a factor of 2, as shown in figure 5b.

The Naval Research Laboratory at the Spatial Warfare Systems Center—San Diego (SSC—SD) has the capability to measure accurately the elastic properties of materials by using a broadband technique developed by Sheiba (1996). Older techniques are more cumbersome and less reliable. The frequency of measurement ranges from subsonic to *ca.* 15 kHz. The measurements are performed in air inside an environmental chamber. Figure 5 also shows the block diagram of the instrumental set-up for these measurements.

The network analyser sends sweeping signals to the shaker. The transducer (sometimes called an accelerometer) and impedance head record the velocities at the base and at the top of the sample. After recording data during this frequency sweep, a new set of data is then obtained at a new temperature setting. Commonly temperatures can range from $-30°$ to $70 °C$. The velocity record constitutes the transfer matrix. By mathematically
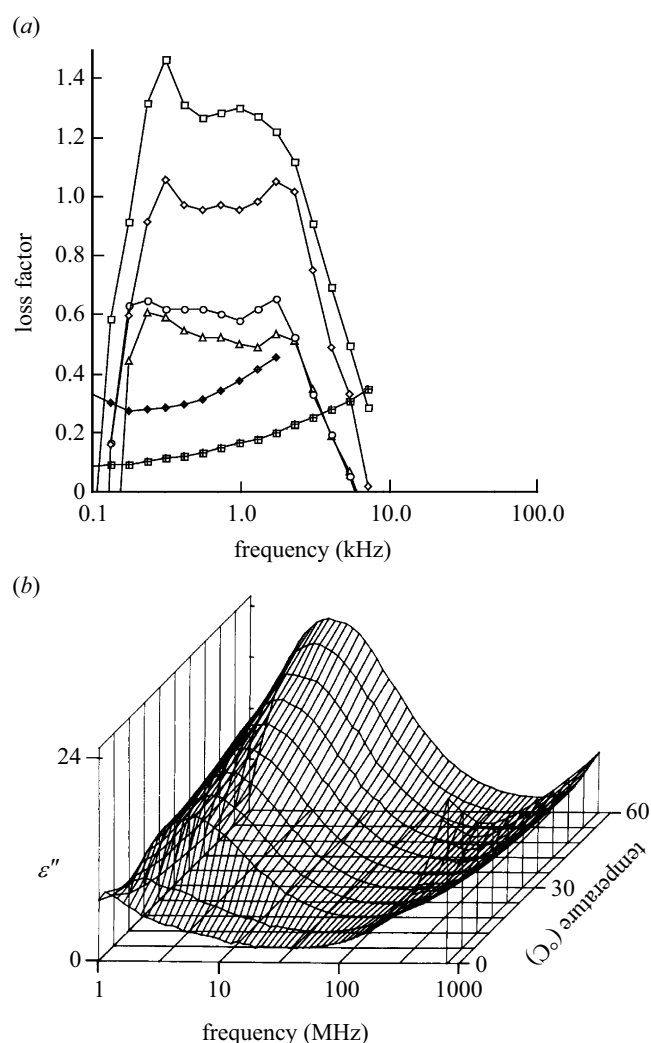
(a)

(b)

(a)

(b)

Figure 6. (a) Plots of the loss factor (absorption per unit volume) for a series of elastomers. Crossed squares represent the curve for natural rubber, and filled diamonds that of the structureless curve for polyurethane, which is recognized as a rubber with a high loss factor in the acoustic absorption range. The upper four curves are for 20 Mrad cross-linked (GVGVP)$_{260}$ (open squares, 20 °C; open diamonds, 10 °C; open circles, 0 °C; open triangles, −5 DC). As the temperature rises above the temperature for the inverse temperature transition of hydrophobic folding and assembly for this composition, the intensity for a localized relaxation grows dramatically. To the best of our knowledge, these model elastic protein-based polymers exhibit the greatest sound absorption for the 100–1000 Hz frequency range. This demonstrates the formation of a regular structure for (GVGIP)$_n$ in contrast to the lack of a regular structure for the classical rubbers. (b) The imaginary (absorptive) section of the dielectric permittivity of poly(GVGIP). The same phenomenon of increased absorption on passing through the temperature range of the inverse temperature transition is observed in the 1–100 MHz range as exhibited by the same composition in the acoustic absorption range. Reproduced, with permission, from Buchet *et al.* (1988). Such low frequency motions provide a source of entropic elasticity and low energy for the structural state of the elastic protein-based polymers.
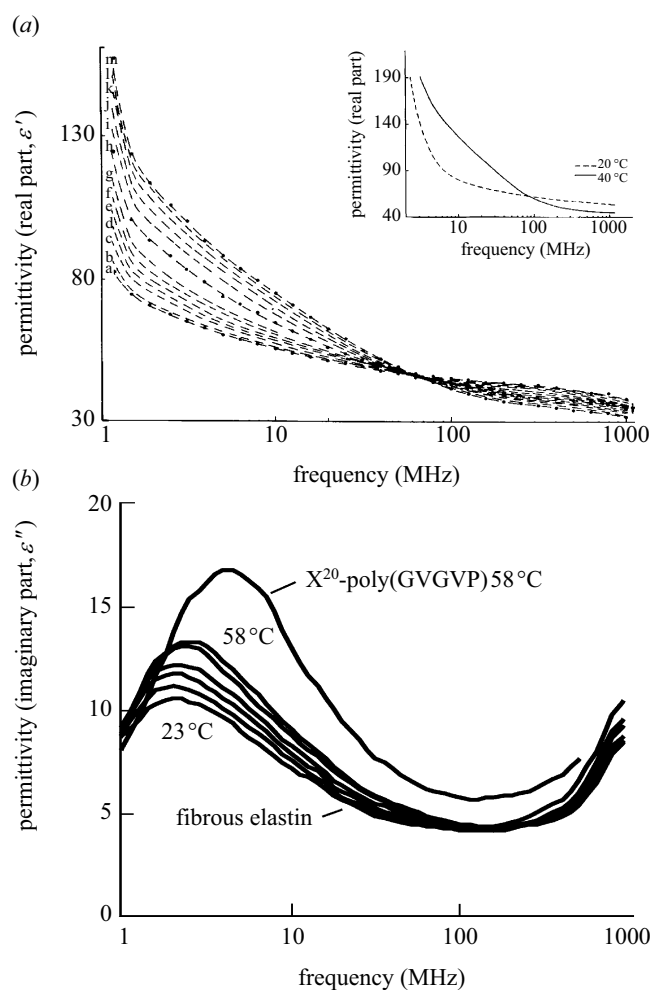
Figure 7. (a) The real part of the dielectric permittivity of α-elastin showing increasing relaxation intensity at *ca.* 5 MHz with increasing temperature from below to above the temperature range for the inverse temperature transition. The data for α-elastin are nearly identical to that found for the polypentapeptide of elastin, poly(GVGVP) shown in the inset for a single temperature below (20°) and one above (40°) that of the inverse temperature transition. The temperatures for the α-elastin data on the left edge of the curves listed as (a)–(m) are 68, 12.5, 20, 25, 30, 35, 40, 45, 50, 55, 60, 65 and 70 °C, respectively. This demonstrates that the same relaxation occurs in a fragment of the natural elastic fibre as has been so thoroughly characterized in the model elastic protein, poly(GVGVP). Reproduced, with permission, from Urry *et al.* (1985a).
(b) The imaginary (absorptive) part of the dielectric permittivity of natural fibrous elastin showing an increasing relaxation at *ca.* 5 MHz with increasing temperature from below (23 °C) to above (58 °C) the temperature range for the inverse temperature transition. The same relaxation is seen at 58 °C with a somewhat higher intensity and a slightly higher frequency is found for the 20 Mrad cross-linked poly(GVGVP). It seems quite evident that dynamic structured states occur in the natural elastic fibre as demonstrated for the model elastic protein-based polymer. Adapted, with permission, from Luan *et al.* (1988).

inverting the transfer matrix, it is possible to extract the complex modulus and Poisson ratio. These data provide a complete description of a material's elastic properties. Further analysis yields the shear modulus, μ, the Poisson ratio, ν, and the loss factor, η, each as a function of frequency and temperature. The loss factor, η, is the main parameter of interest. It represents the energy absorption per unit volume at a given frequency. The loss factor versus frequency and temperature were determined for several different elastic protein-based polymer compositions. The data for $(GVGIP)_{nx260}$ are given in figure 6a. MATHCAD 7.0 was used to perform the mathematical analysis.

(ii) *Comparison of the acoustic absorptions of (GVGIP) and natural rubber*

Natural rubber has been well characterized as a random-chain network. This means that there are no regular repeating conformational features in the polymer chain. The consequence of a random chain is a broad, slowly changing dependence on frequency of physical properties, such as absorption. Simply stated, the absence of structure means that the barrier to rotation about each bond will tend to be different. This is what is observed in figure 6a for natural rubber and a synthetic petroleum-based polymer, polyurethane, chosen for its relatively high loss factor in the frequency range reported.

At frequencies lower than those of the IR spectroscopic range, however, any material that exhibits a localized absorption band as a function of frequency must do so by virtue of a regular repeating structure. Interestingly, this is seen in Figure 6a for X^{20}-$(GVGIP)_{260}$ in the range 200 Hz to 7 kHz, and the intensity of the absorption per unit volume increases as the temperature is raised through the temperature interval of the inverse temperature transition. Acoustic absorption increases as the structure becomes more regular! Besides demonstrating the remarkable acoustic absorption property of this material, the acoustic absorption data provide an additional demonstration of the existence of a regular structure for poly(GVGIP) and for related polymers. Actually, this is simply further confirmation of earlier dielectric relaxation data, which demonstrated the development of an intense localized relaxation at *ca.* 5 MHz as the temperature was raised through the interval of the inverse temperature transition, as reviewed below.

(c) *Previous dielectric relaxation studies on elastin-related systems*

(i) *Dielectric relaxation and acoustic absorption data on the same polymer*

Figure 6b is a three-dimensional plot of the imaginary (absorption) part of the dielectric permittivity of poly(GVGIP) as a function of frequency and temperature. Just as for the acoustic absorption study in figure 6a, there is an increase in the absorption (imaginary) component of the dielectric relaxation as the temperature rises through the temperature interval of the inverse temperature transition for hydrophobic folding and assembly. Thus, the data on the elastin models can now be directly compared to α-elastin and fibrous elastin, itself. Mechanical resonances due to regularly repeating structures have now been observed both in the vicinities of 1 kHz and 5 MHz.

(ii) *Comparison of poly(GVGVP) and α-elastin*

Figure 7a is a graph of the real part of the dielectric permittivity as a function of temperature for α-elastin and for poly(GVGVP) in the inset. In both cases, there is development of an intense relaxation at *ca.* 5 MHz as the protein-based elastomers hydrophobically fold and assemble on increasing the temperature through the range of the inverse temperature transition. Both elastomeric molecular systems exhibit the same development of regular structure on raising the temperature through the range of the inverse temperature transition.

(iii) *Comparison of cross-linked poly(GVGVP) to fibrous elastin*

Figure 7b is a graph of the imaginary (absorption) part of the dielectric relaxation for purified fibrous elastin (from bovine ligamentum nuchae) as a function of temperature from 23 °C to 58 °C. Figure 7b also contains a plot of the same data at 58 °C for the elastomer, 20 Mrad cross-linked poly(GVGVP). While there is a small increase in mean frequency and intensity for the X^{20}-$(GVGVP)_{251}$ relaxation, it is certain that there is hydrophobic folding and assembly resulting in the formation of regular structures in the natural fibrous elastin that are similar to those of cross-linked poly(GVGVP). Incidentally, the decrease in intensity at 1 GHz for fibrous elastin reflects the loss of hydrophobic hydration as the hydrophobic folding proceeds. This is due to a dielectric relaxation at *ca.* 5 GHz, which results from hydrophobic hydration (Urry *et al.* 1997).

4. DISCUSSION

(a) *Relevance of proposed mechanisms for the entropic (ideal) elasticity of elastin*

The kernel of the classical theory of rubber elasticity originated with K. H. Meyer in 1932 which, according to Flory (1968, p. G42), can be stated as '... the orientation of the molecules of a piece of rubber when it is stretched would entail a decrease in entropy, and thus could account for the retractive force.' This was restated by Flory (1968) in terms of two subsidiary hypotheses: (i) the restoring force originates within the chain molecules by distortion of the distribution of their configurations and not from interactions between chains; and (ii) the restoring force is due 'exclusively to the *entropy* of the chain configuration'. However, is the alignment of chains really the most appropriate description of entropic elasticity? Even in the case of a bulk elastomer, might the most fundamental statement be the decrease in internal chain dynamics within each chain, which would be fundamental to the alignment of elongation? Clearly, the above-demonstrated entropic elasticity exhibited by a single chain does not arise from the alignment of many chains on extension. Rather, the observation of entropic elasticity on extension of a single chain fixed at its ends limits the source of entropy change to the damping of internal chain dynamics within the single chain. In this case entropic elasticity cannot arise from the change in relative orientation of many chain molecules.
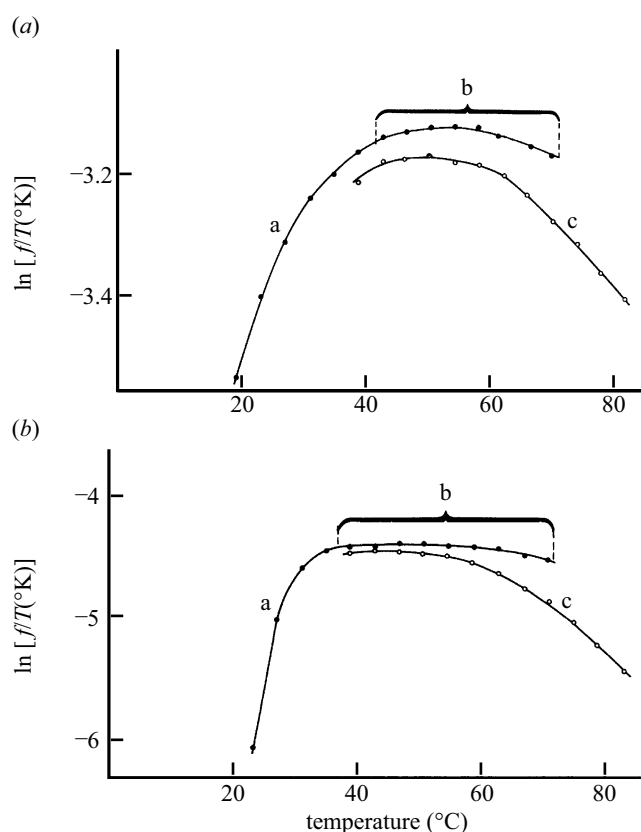
(a)

(b)

Figure 8. Thermoelasticity curves for *(a)* fibrous elastin and *(b)* 20 Mrad cross-linked poly(GVGVP). See text for discussion. Whether or not a near-zero slope, i.e. an $f_E/f \ll 1$, is obtained depends on the rate at which the temperature is raised. This is due to a slow denaturation at temperatures above 60 °C. (Times per data point for line segments (a), (b) and (c) are 4 h, 30 min and 4 h, respectively.) Reproduced, with permission, from Urry (1988*a,b*).

(i) *Relevance of the Flory random-chain network theory of entropic elasticity*

Flory's publications describe a Gaussian distribution of end-to-end chain lengths that results from a random-chain network, and they assert that the decrease in entropy due to extension, or compression, arises from distortion of the network from this most probable random distribution (Flory 1953, 1968). Hoeve & Flory (1958, 1974) concluded that the entropic elasticity of elastin arises from such a random-chain network.

There are four principal reasons why this perspective is questionable. These are (i) a limited potential for cross-links in the fixed sequence of elastin, (ii) the above spectroscopic evidence for regular, non-random, dynamic structural features in components of elastin, (iii) the above report of the occurrence of ideal reversible elasticity exhibited by a single chain of repeat sequences of elastin with calculated single-chain elastic moduli similar to the macroscopic elastic modulus, and (iv) an irreversible loss of force due to thermal denaturation when the elastomer is extended and heated at temperatures above 60 °C.

Relevance of the probability of cross-link formation to structure

In rubber, each repeating unit is a potential cross-link, and, on vulcanization, any pair of repeating units can be converted to a cross-link wherever two chain segments are sufficiently proximal. In elastin, only lysine residues form the cross-links, and yet there are only some 40 lysine residues for an elastin protein of *ca.* 800 residues, i.e. one lysine in every 20 residues. Furthermore, the lysine residues are arranged in an orderly manner along the sequence. Most commonly, four lysine residues combine to form a single cross-link, called a desmosine, and essentially all of the lysine residues in fibrous elastin have been formed into cross-links. Such cross-linking cannot be achieved within a random-chain network. The achievement of such rare cross-linkages requires elements of order (Urry 1976).

Low-frequency motions provide much entropy to chain structures

Motions that are due to rotations about backbone bonds in a chain molecule that exhibit intense relaxations limited to localized frequency intervals, that is, intense mechanical resonances, can only result from polymers containing regular, non-random, dynamic structures. For model elastin systems including purified fibrous elastin, such mechanical relaxations are observed at *ca.* 1 kHz and 5 MHz (see figures 6 and 7). As will be demonstrated below, these relaxations provide a very ample source of entropy to structured elastin systems. These contributions to entropy increase greatly as the frequency of the relaxation is lower, and they are contributions to the free energy of protein structure that have yet to be adequately treated in the current computations of low-energy protein structures. Most importantly for entropic elasticity, low-frequency motions provide an abundant and ready source of entropy decrease on extension.

Entropic elastomeric force arising from a single chain

At a fixed extension in the AFM single-chain force–extension curves of figure 3, there is a single end-to-end chain length. The entropic elastic force measured at a given extension cannot have arisen from displacement of a network of chains from a Gaussian distribution of end-to-end chain lengths nor can it arise from aligning chains in parallel. The decrease in entropy that provides the entropic restoring force in the single-chain experiment must arise from a damping of internal chain dynamics of the single chain. No other degrees of freedom can cause a decrease in chain entropy to occur. Furthermore, in order that the ends of the chain remain fixed in space, the rotation about a given bond must be compensated for by a corresponding correlated rotation about one or more additional bonds. The peptide librational mechanism of entropic elasticity, which arises so readily out of the β-spiral structure of poly(GVGVP) represents one interesting means of achieving this.

Studies of the temperature dependence of force at a fixed extension have yet to be carried out on single chains in order to determine the contribution of internal energy or the enthalpy component of the force, i.e. to determine the f_E/f ratio as given in equations (1.7) and (1.8). In respect of the internal energy or enthalpic contribution to

(a)

(b)   β-turn

(c)
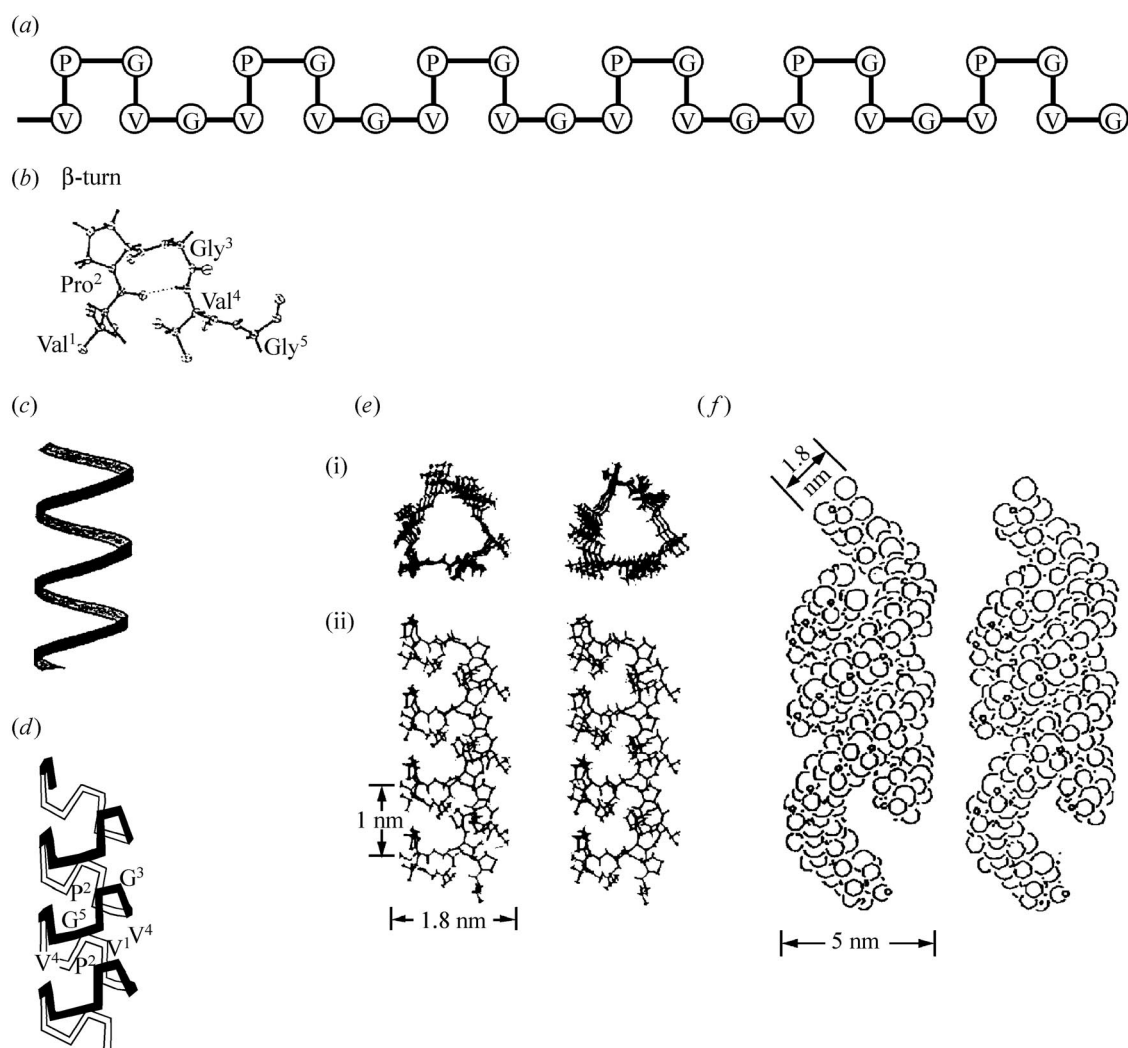
(d)

(e)

(i)

(ii)

1 nm

1.8 nm

(f)

1.8 nm

5 nm

Figure 9. Description of the proposed molecular structure of poly(GVGVP). (a) Schematic representation of the repeating Pro-Gly-containing sequence inserting the β-turn structure, which is given in crystallographic detail in part (b). (c) Schematic helical representation of the structure that forms on raising the temperature above the inverse temperature transition. (d) Schematic representation of the helical structure, called a β-spiral, but with the β-turns included and functioning as spacers between turns of the helix. (e) Stereo pairs of the β-spiral structure in atomic detail in (i) end view and (ii) side view. (f) Associated β-spirals having formed multi-stranded twisted filaments, which is the more accurate description of the hydrophobically folded and assembled state.

the elastic force, these would arise reversibly without bond breakage, by strain-imposed distortions in bond lengths and bond angles. Interestingly, Young (private communication) probed the strain deformation of silk fibres (*Bombyx mori* and spider dragline) using Raman spectroscopy and observed, among other spectral changes, a shift in the 1095 cm^{-1} (wavenumber) band on extension to 3.5%. This band shift, assigned to the C–C stretch mode, represents an internal energy component to the force. Provided that the stretch is reversible with no bond breakage, it can contribute to the force of an ideal elastomer.

At high extensions, where the force resulting in bond deformations can become significant, however, distortions in bond lengths and bond angles can decrease the durability of an elastic fibre by chain rupture. In this regard, the remarkable feature of the mammalian elastic fibre is its striking durability where, in the aortic arch and descending thoracic aorta, the half-life is some 70 years

during which period the elastic fibres will have undergone more than one billion stretch–relaxation cycles. This is possible due to the dominantly entropic nature of its elastic force as seen in figure 8b and due to uniform chain extension arising out of a regular, cross-linked structure where no single chain bears an excessive amount of the load.

Loss of elastomeric force of elastin-based systems due to thermal denaturation

In figure 1, it was noted that poly(GVGVP) exhibits a slow irreversible denaturation when held at temperatures above 60 °C. This same phenomenon is apparent in the thermoelasticity studies on fibrous elastin, as originally noted by Dorrington & McCrum (1977). In the thermoelasticity experiments illustrated in figure 8 (Urry 1988a,b), the elastomer is equilibrated at 40 °C and at that temperature is extended to 60%. At this fixed length, the temperature is lowered to *ca.* 20 °C and slowly raised

to 80 °C. The force dramatically increases as the temperature is raised through the range of the inverse temperature transition from 20 to 40 °C. Then, the force/T (°K) tends to remain nearly constant from 40 to 60 °C, especially for X^{20}–poly(GVGVP). The value of lnf/T begins to decrease above 60 °C in a time-dependent manner. When using a rate of increase of 4 °C 30 min^{-1}, 8 °C h^{-1}, there is a decrease in lnf/T, and, when the temperature is returned to 40 °C, an irreversible loss of force occurs. The decrease in force above 60 °C is more dramatic on raising the temperature more slowly, e.g. when raising the temperature at a rate of 1 °C h^{-1}. When the temperature maintained above 60 °C for a longer interval irreversible thermal denaturation is seen most dramatically. Furthermore, a plot of ln(elastic modulus) versus time at 80 °C is linear, providing evidence of a first order process (Urry 1988*a*,*b*). Interestingly, while heating above 60 °C decreases force, it also shortens the length at which zero force is obtained, as is to be expected when a filamentous, β-spiral-like structure becomes randomized by thermal denaturation.

As discussed in relation to equations (1.7) and (1.8), a slope of zero for plots like those in figure 8 would mean an ideal (entirely entropic) elastomer. As clearly seen for X^{20}–poly(GVGVP) in the 40–60 °C temperature range, when data are collected at the rate of 30 min per data point, a near-zero slope is obtained. Commonly, an f_E/f ratio of 0.1 is obtained for X^{20}–poly(GVGVP) (Luan *et al.* 1989). Because of the steep positive slope between 20 and 40 °C, due to the hydrophobic folding and assembly of the inverse temperature transition, and because of the slow irreversible thermal denaturation above 60 °C, the slope, obtained in the thermoelasticity experiment from which the entropic contribution is estimated, depends on the rate at which the data are collected and the temperature interval over which they are collected.

A steep rise in force in the 20–40 °C temperature interval for fibrous elastin in figure 8*a*, although less steep than that seen in figure 8*b* for X^{20}–poly(GVGVP), demonstrates the effect of the inverse temperature transition within elastin itself. More dramatic for fibrous elastin is the loss of elastomeric force on raising the temperature above 60 °C. This finding, of a slow loss of force at elevated temperature, would not have been so apparent if the time had been limited to a single day to perform the experiment (without the advantage of computerized equipment), as was the case when Hoeve & Flory (1958) carried out their original study on fibrous elastin. For the thermoelasticity study of fibrous elastin shown in figure 8, however, the rate of loss of force at elevated temperature is even greater than for X^{20}–poly(GVGVP).

Additionally, the plot of ln(elastic modulus) versus time for fibrous elastin maintained at 80 °C, as determined by a stress–strain curve every 24 h, is a straight line with a half-life of *ca*. 10 days (Urry 1988*b*). Another important feature of the data for determining half-life is that the length at which zero force is obtained decreases with time at 80 °C. Remarkably, this means that the loss of force in figure 8, and the progressive loss of elastic modulus exhibited by a series of stress–strain curves after heating for 24 h at 80 °C, are not due to structural rearrangement to an extended state under load. Additionally, it cannot be due to slipping of the sample in the grip. Instead, extended time-periods at a high temperature result in a denatur-

ation, which entails a randomization from linear filamentous structures towards denatured random-coil structures. This has an analogy to the loss of percentage water by weight for time above 60 °C in figure 1.

Figure 8 clearly displays, in the thermoelasticity data of elastin-based systems, in the half-life studies for the elastic modulus at 80 °C, and in the structural change above 60 °C in figure 1, a slow thermal denaturation of protein-based elastomers. As random-chain networks do not exhibit thermal denaturation, these elastin-based systems cannot properly be described as random-chain networks. Thus, the evidence is clear and abundant; elastin-based systems contain regular repeating conformations and those ordered structures denature.

(ii) *Relevance of solvent entropy changes as a source of entropic elastic force*

Effect of removing solvent entropy change during the inverse temperature transition

The change in solvent entropy is fundamental to the occurrence of an inverse temperature transition. This transition has been extensively utilized to perform the family of energy conversions that sustain living organisms (Urry 1993, 1997), and therefore the inverse temperature transition is extensively characterized. One approach to testing whether the change in solvent entropy contributes to the elastomeric force is to utilize an approach due to Flory, that is, to reduce the heat of the inverse temperature transition to near zero by an appropriate solvent mixture. Hoeve & Flory (1958) used a mixture of 30% ethylene glycol by weight in water in their thermoelasticity study that deduced a dominant entropic elastic force for fibrous elastin. When Luan *et al.* (1989) compared the thermo-elasticity-derived f_E/f ratio of X^{20}–poly(GVGVP) in water and in 30% ethylene glycol, the values were the same, 0.1. Based on the approximations of equations (1.7) and (1.8), X^{20}–poly(GVGVP) is a dominantly entropic elastomer in both solvent systems. The effect of adding the ethylene glycol is to reduce the heat of the transition to near zero. Now, since the entropy of the desolvation process is the heat of the transition divided by the temperature of the transition, $\Delta H_t/T_t$, the solvent entropy change would be approaching zero, and yet the solvent mixture, instead of reducing the elastomeric force, remarkably, did the opposite and resulted in a substantial increase in force. The conclusion is that there is no experimental basis for believing that solvent entropy change contributed to elastomeric force.

The polymer chains bear the force; solvation changes alter the fraction of chain segments that sustain the force?

The force of deformation must be borne by the chains; it cannot be borne by the solvent. At a fixed length, raising the temperature of a band of elastomer from below to above the temperature of the inverse temperature transition increases the force. Alternatively, increasing the chemical potential to lower the transition temperature from above to below the operating temperature at a fixed length causes an increase in the elastomeric force (Urry 1997; Urry *et al.* 1988*a*,*b*). These results are due to an increase in hydrophobic folding and assembly of the chains. As this is the case at a fixed length, the smaller fraction of a chain's length, which is not folded, must
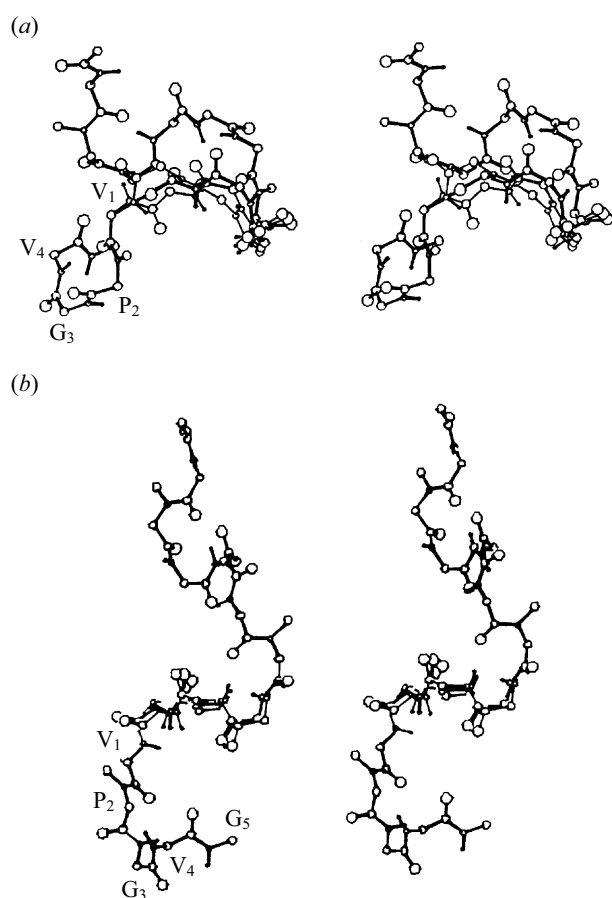
(a)

(b)

Figure 10. Stereo view of the torsional oscillations possible within a 2 kcal mol^{-1} residue cut-off energy for the central pentamer of one turn (three pentamers) of the β-spiral structure of poly(GVGVP) (a) in the relaxed state and (b) in the 130% extended state. See text for discussion. Reproduced, with permission, partly from Urry *et al.* (1982) and the remainder from Urry *et al.* (1985c).

necessarily be further extended. Accordingly, in order to maintain a fixed length, the unfolded segments must be further extended. This provides for the increase in entropic elastic force by means of a decrease in configurational entropy.

(iii) *Entropic elasticity due to damping of internal chain dynamic on extension*

Molecular structure of poly(GVGVP)

In order to understand the concept of the damping of internal chain dynamics on extension, the structure given in figure 9 is helpful. The Pro–Gly-containing elastomeric sequential polypeptides exhibit a repeating β-turn structure as schematically shown in figure 9a, and the β-turn is given in crystallographic detail in figure 9b. A rise in the temperature of the inverse temperature transition results in the optimization of intra- and intermolecular hydrophobic association. Intramolecularly, this results in a helical structure called a β-spiral, which is shown schematically as a helix in figure 9c, in more detail, with β-turns schematically shown as spacers between turns of the helix, in figure 9d, and in atomic stereo detail in figure 9e. Intermolecularly, the β-spirals associate to form multistranded twisted filaments, as depicted in figure 9f.

Because there is water within the β-spiral, and as a result of the β-turns functioning as spacers, the peptide segments connecting β-turns are free to undergo large amplitude torsional oscillations.

Effect of extension on the amplitude of the torsional oscillations and on chain entropy

The magnitude of the torsional (dihedral angle) excursions for a single pentamer sandwiched within a turn of β-spiral (three pentamers) for a 1.5 kcal mol^{-1} residue cut-off energy is shown in figure 10a when using the molecular mechanics calculations of the Scheraga approach (Momany *et al.* 1975). Dihedral angle oscillations of 160° are possible. The effect of a 130% extension of the β-spiral pitch, shown in figure 10b, is a dramatic decrease in the amplitude of the torsional oscillations allowed within a 1.5 kcal mol^{-1} residue cut-off energy. Using an enumeration of states approach with each change of 5° in any single torsion angle counted as a new state, the decrease in numbers of states for a 0.6 kcal mol^{-1} residue cut-off energy (i.e. within an energy cut-off of RT) is from a W^r of 342 to a W^e of 24. Using equation (1.10), this gives a value for ΔS of -5.28 cal mol^{-1} deg^{-1} per pentamer. If the Boltzmann summation over all energies is used, the value is -5.06 cal mol^{-1} deg^{-1} per pentamer (Urry *et al.* 1985c).

Alternatively, when using the molecular dynamics approach of Karplus, the expression becomes

$$\Delta S = R \ln[\Pi_i \Delta \phi_i^e \Delta \psi_i^e / \Pi_i \Delta \phi_i^r \Delta \psi_i^r], \qquad (3.1)$$

where the product Π_i is over the rms torsion angle fluctuations $\Delta \phi_i^e$ and $\Delta \psi_i^e$ for the extended state divided by the product of the rms torsion angle fluctuations $\Delta \phi_i^r$ and $\Delta \psi_i^r$ for the relaxed state as obtained from the molecular dynamics trajectories for the relaxed and 130% extended states. The calculated decrease in entropy was -5.5 cal mol^{-1} deg^{-1} per pentamer for the 130% extension (Chang & Urry 1989). Whether the calculation of entropy is by means of an enumeration of states in ψ–ϕ configuration space or the amplitude of the torsional oscillations in a molecular dynamic simulation, the calculated entropy change for a 130% extension is the same.

Calculation of contribution of force due to decrease in freedom of motion on extension

From equations (1.4) and (1.5) we have

$$f_S = T(\partial S/\partial L)_{V,T}. \qquad (3.2)$$

At physiological temperatures, 310 K, and for an extension from 0.35 to 0.8 nm for a pentamer within the β-spiral structure of figure 9e with a calculated decrease in entropy of 5 cal mol^{-1} deg^{-1} per pentamer, the calculated value for the entropic contribution to the elastomeric force is 24 pN for a single chain of β-spiral.

To put this in terms of an elastic modulus in units of N m^{-2}, it is necessary to estimate the number of β-spirals per m^2. From figure 1, the functional state is 37% peptide by weight. Taking the density of the peptide to be 1.33 g cm^{-3}, and a cross-sectional area of 3.2 nm^2 per β-spiral, there would be *ca.* 8.7×10^{16} parallel-aligned β-spirals per m^2. The calculated result is 2×10^6 N m^{-2}, which is an order of magnitude larger than the

experimental value of 1.6×10^5 N m^{-2} for 20 Mrad cross-linked (GVGVP)$_{251}$.

Several obvious factors can be considered, that would contribute to a higher calculated value for the elastic modulus of the isolated β-spiral than for the experimental elastic modulus of the cross-linked matrix. First, in the cross-linked matrix the β-spirals would be randomly orientated with respect to the direction of extension. Second, the β-spirals occur as part of a multistranded twisted filament as shown in figure 9*f*, which would tend to dampen the torsional oscillations within the triple-stranded filament and thereby result in a lower entropy change on extension. Thus, it would seem that the damping of internal chain dynamics on extension provides abundant entropic restoring force in elastin-based systems. Furthermore, given the entropic elasticity of single chains demonstrated by the AFM single-chain force–extension curves, damping of internal chain dynamics on extension should be considered, in general, as a potential fundamental source for the development of entropic elastic force in chain molecules.

(iv) *Dependence of entropy and structural free energy on oscillator frequency*

One final point for consideration in this report is the significance of the occurrence of intense low-frequency mechanical motions in elastin-based systems. The insight comes from the expression for the dependence of entropy on oscillator frequency. From the expression for the partition function of the harmonic oscillator (Dauber *et al.* 1981), it is seen that the slope for the frequency dependence of entropy is -4.6 EU $\log \nu_i^{-1}$. The extrapolation of the harmonic oscillator treatment to low-frequency torsional oscillations is surely not quantitative, but it is nonetheless informative. While the contribution of a lower classical vibration frequency is of the order of 5 cal mol^{-1} deg^{-1} (EU), giving a Gibbs free energy of 1.5 kcal mol^{-1} at 298 K, the contribution of the 5 MHz relaxation, seen in figures 6 and 7, would approach 30 cal mol^{-1} deg^{-1} or 9 kcal mol^{-1}, and that for the mechanical resonance at *ca.* 1 kHz, reported in figure 6*a*, would approach 47 cal mol^{-1} deg^{-1} or 14 kcal mol^{-1}. From this it should be apparent that these relaxations are fundamental in providing for the entropic elasticity of elastin-based systems. On a more general note, computations of protein structure that do not include these important low-frequency contributions to the free energy would seem to be limited in their treatment of the structure–function issue.

REFERENCES

Buchet, R., Luan, C.-H., Prasad, K. U., Harris, R. D. & Urry, D. W. 1988 Dielectric relaxation studies on analogs of the polypentapeptide of elastin. *J. Phys. Chem.* **92**, 511–517.

Bustamante, C., Marko, J. F., Siggia, E. D. & Smith, S. 1994 Entropic elasticity of lambda-phage DNA. *Science* **265**, 1599–1600.

Butt, H. J. & Jaschke, M. 1995 Calculation of thermal noise in atomic force microscopy. *Nanotechnology* **6**, 1–7.

Chang, D. K. & Urry, D. W. 1989 Polypentapeptide of elastin: damping of internal chain dynamics on extension. *J. Comput. Chem.* **10**, 850–855.

Clausen-Schaumann, H., Rief, M., Tolksdorf, C. & Gaub, H. E. 2000 Mechanical stability of single DNA molecules. *Biophys. J.* **78**, 1997–2007.

Cleveland, J. P., Manne, S., Bocek, D. & Hansma, P. K. 1993 A nondestructive method for determining the spring constant of cantilevers for scanning force microscopy. *Rev. Sci. Instrum.* **64**, 403–405.

Cook, W. J., Einspahr, H. M., Trapane, T. L., Urry, D. W. & Bugg, C. E. 1980 Crystal structure and conformation of the cyclic trimer of a repeat pentapeptide of elastin, cyclo-(L-valyl-L-prolylglycyl-L-valylglycyl)$_3$. *J. Am. Chem. Soc.* **102**, 5502–5505.

Cox, B. A., Starcher, B. C. & Urry, D. W. 1973 Coacervation of α-elastin results in fiber formation. *Biochim. Biophys. Acta* **317**, 209–213.

Cox, B. A., Starcher, B. C. & Urry, D. W. 1974 Coacervation of tropoelastin results in fiber formation. *J. Biol. Chem.* **249**, 997–998.

Dauber, P., Goodman, M., Hagler, A. T., Osguthorpe, D., Sharon, R. & Stern, P. 1981 In *ACS Symp. Ser. No. 173. Suypercomputers in chemistry* (ed. P. Lykos & I. Shavitt), pp. 161–191. Washington, DC: American Chemical Society.

Dorrington, K. L. & McCrum, N. G. 1977 Elastin as a rubber. *Biopolymers* **16**, 1201–1222.

Eyring, H., Henderson, D., Stover, B. J. & Eyring, E. M. 1964 *Statistical mechanics and dynamics.* New York: Wiley.

Flory, P. J. 1953 *Principles of polymer chemistry.* Ithaca, NY: Cornell University Press.

Flory, P. J. 1968 Molecular interpretation of rubber elasticity. *Rubber Chem. Technol.* **41**, G41–G48.

Flory, P. J., Ciferri, A. & Hoeve, C. A. J. 1960 The thermodynamic analysis of thermoelastic measurements on high elastic materials. *J. Polymer Sci.* **XLV**, 235–236.

Gotte, L., Giro, G., Volpin, D. & Horne, R. W. 1974 The ultrastructural organization of elastin. *J. Ultrastruct. Res.* **46**, 23–33.

Grinberg, N. V., Dubovik, A. S., Grinberg, V. Y., Kuznetsov, D. V., Makhaeva, E. E., Grosberg, A. U. & Tanaka, T. 1999 Studies of the thermal volume transition of poly(N-isopropylacrylamide) hydrogels by high sensitivity differential scanning microcalorimetry. 1. Dynamic effects. *Macromolecules* **32**, 1471–1475.

Hoeve, C. A. J. & Flory, P. J. 1958 The elastic properties of elastin. *J. Am. Chem. Soc.* **80**, 6523–6526.

Hoeve, C. A. J. & Flory, P. J. 1962 Elasticity of crosslinked amorphous polymers in swelling equilibrium with diluents. *J. Polymer Sci.* **60**, 155–164.

Hoeve, C. A. J. & Flory, P. J. 1974 Elastic properties of elastin. *Biopolymers* **13**, 677–686.

Li, B., Alonso, D. O. V. & Daggett, V. 2000 The molecular basis for the inverse temperature transition of elastin. *J. Mol. Biol.* **305**, 581–592.

Luan, C.-H., Harris, R. D. & Urry, D. W. 1988 Dielectric relaxation studies on bovine ligamentum nuchae. *Biopolymers* **27**, 1787–1793.

Luan, C.-H., Jaggard, J., Harris, R. D. & Urry, D. W. 1989 On the source of entropic elastomeric force in polypeptides and proteins: backbone configurational vs side chain solvational entropy. *Int. J. Quant. Chem. Quant. Biol. Symp.* **16**, 235–244.

Manno, M., Emanuele, A., Martorana, V., San Biagio, P. L., Bulone, D., Palma-Vitorelli, M. B., McPherson, D. T., Xu, J., Parker, T. M. & Urry, D. W. 2001 Interaction of processes on different time scales in a bioelastomer capable of performing energy conversion. *Biopolymers* **59**, 51–64.

Odijk, T. 1995 Stiff chains and filaments under tension. *Macromolecules*, **28**, 7016–7018.

Oesterhelt, F., Rief, M. & Gaub, H. E. 1999 Single molecule force spectroscopy by AFM indicates helical structure of poly(ethylene-glycol) in water. *New J. Phys.* **1**, 6.

Partridge, S. M. 1966 Biosynthesis and nature of elastin structures. *Federation Proc.* **25**, 1023–1029.

Partridge, S. M. 1967 Diffusion of solutes in elastin fibers. *Biochim. Biophys. Acta* **140**, 132–141.

Partridge, S. M. & Davis, H. F. 1955 The chemistry of connective tissues. II. Composition of soluble proteins derived from elastin. *Biochem. J.* **61**, 21–30.

Partridge, S. M., Davis, H. F. & Adair, G. S. 1955 The chemistry of connective tissues. II. Soluble proteins derived from partial hydrolysis of elastin. *Biochem. J.* **61**, 11–21.

Rief, M., Oesterhelt, F., Heymann, B. & Gaub, H. E. 1997 Single molecule force spectroscopy on polysaccharides by atomic force microscopy science. *Science* **275**, 1295–1297.

San Biagio, P. L., Madonia, F., Trapane, T. L. & Urry, D. W. 1988 Overlap of elastomeric polypeptide coils in solution required for single phase initiation of elastogenesis. *Chem. Phys. Lett.* **145**, 571–574.

Sciortino, F. K., Prasad, K. U., Urry, D. W. & Palma, M. U. 1993 Self-assembly of bioelastomeric structures from solutions: mean field critical behavior and Flory–Huggins free-energy of interaction. *Biopolymers* **33**, 743–752.

Sheiba, L. 1996 Broad band method and apparatus for the precise measurement of the complex modulus of viscoelastic materials. US patent 08/645,878, pending.

Urry, D. W. 1976 On the molecular mechanisms of elastin coacervation and coacervate calcification. *Farad. Discuss. Chem. Soc.* **61**, 205–212.

Urry, D. W. 1988a Entropic elastic processes in protein mechanisms. I. Elastic structure due to an inverse temperature transition and elasticity due to internal chain dynamics. *J. Protein Chem.* **7**, 1–34.

Urry, D. W. 1988b Entropic elastic processes in protein mechanism. II. Simple (passive) and coupled (active) development of elastic forces. *J. Protein Chem.* **7**, 81–114.

Urry, D. W. 1993 Molecular machines: how motion and other functions of living organisms can result from reversible chemical changes. *Angew. Chem.* **105**, 859–883 [in German]; *Angew. Chem. Int. Edn* **32**, 819–841 [in English].

Urry, D. W. 1997 Physical chemistry of biological free energy transduction as demonstrated by elastic protein-based polymers. *J. Phys. Chem. B* **101**, 11 007–11 028.

Urry, D. W., Long, M. M. & Sugano, H. 1978 Cyclic analog of elastin polyhexapeptide exhibits an inverse temperature transition leading to crystallization. *J. Biol. Chem.* **253**, 6301–6302.

Urry, D. W., Venkatachalam, C. M., Long M. M. & Prasad, K. U. 1982 Dynamic β-spirals and a librational entropy mechanism of elasticity. In *Conformation in biology*, G. N., Ramachandran Festschrift vol. (ed. R. Srinivasan & R. H. Sarma), pp. 11–27. Guilderland, NY: Adenine Press.

Urry, D. W., Wood, S. A., Harris, R. D. & Prasad, K. U. 1984 Polypentapeptide of elastin as an elastomeric biomaterial. In *Polymers as biomaterials* (ed. S. W. Shalaby, T. Horbett, A. S. Hoffman & B. Ratner), pp. 17–32. New York: Plenum Press.

Urry, D. W., Henze, R., Redington, P., Long, M. M. & Prasad, K. U. 1985a Temperature dependence of dielectric relaxations in α-elastin coacervate: evidence for a peptide librational mode. *Biochem. Biophys. Res. Commun.* **128**, 1000–1006.

Urry, D. W., Trapane, T. L. & Prasad, K. U. 1985b Phase-structure transitions of the elastin polypentapeptide–water system within the framework of composition–temperature studies. *Biopolymers* **24**, 2345–2356.

Urry, D. W., Venkatachalam, C. M., Wood, S. A. & Prasad, K. U. 1985c Molecular structures and librational processes in sequential polypeptides: from ion channel mechanisms to bioelastomers. In *Structure and motion: membranes, nucleic acids and proteins* (ed. E. Clementi, G. Corongiu, M. H. Sarma & R. H. Sarma), pp. 185–203. Guilderland, NY: Adenine Press.

Urry, D. W., Haynes, B., Zhang, H., Harris, R. D. & Prasad, K. U. 1988a Mechanochemical coupling in synthetic polypeptides by modulation of an inverse temperature transition. *Proc. Natl Acad. Sci. USA* **85**, 3407–3411.

Urry, D. W., Harris, R. D. & Prasad, K. U. 1988b Chemical potential driven contraction and relaxation by ionic strength modulation of an inverse temperature transition. *J. Am. Chem. Soc.* **110**, 3303–3305.

Urry, D. W., Peng, S. Q., Xu, J. & McPherson, D. T. 1997 Characterization of waters of hydrophobic hydration by microwave dielectric relaxation. *J. Am. Chem. Soc.* **119**, 1161–1162.

Vrhovski, B., Jensen, S. & Weiss, A. S. 1997 Coacervation characteristics of recombinant human tropoelastin. *Eur. J. Biochem.* **250**, 92–98.

Volpin, D., Urry, D. W., Pasquali-Ronchetti, I. & Gotte, L. 1976 Studies by electron microscopy on the structure of coacervates of synthetic polypeptides of tropoelastin. *Micron* **7**, 193–198.

Weis-Fogh, T. & Andersen, S. O. 1970 New molecular model for the long-range elasticity of elastin. *Nature* **227**, 718–721.

Wu, W. J., Vrhovski, B. & Weiss, A. S. 1999 Glycosaminoglycans mediate the coacervation of human tropoelastin through dominant charge interactions involving lysine side chains. *J. Biol. Chem.* **274**, 21 719–21 724.